

NANO EXPRESS

Open Access

Controlled atom transfer radical polymerization of MMA onto the surface of high-density functionalized graphene oxide

Mukesh Kumar, Jin Suk Chung and Seung Hyun Hur*

Abstract

We report on the grafting of poly(methyl methacrylate) (PMMA) onto the surface of high-density functionalized graphene oxides (GO) through controlled radical polymerization (CRP). To increase the density of surface grafting, GO was first diazotized (DGO), followed by esterification with 2-bromoisobutryl bromide, which resulted in an atom transfer radical polymerization (ATRP) initiator-functionalized DGO-Br. The functionalized DGO-Br was characterized by X-ray photoelectron spectroscopy (XPS), Raman, and XRD patterns. PMMA chains were then grafted onto the DGO-Br surface through a 'grafting from' technique using ATRP. Gel permeation chromatography (GPC) results revealed that polymerization of methyl methacrylate (MMA) follows CRP. Thermal studies show that the resulting graphene-PMMA nanocomposites have higher thermal stability and glass transition temperatures (T_g) than those of pristine PMMA.

Keywords: Graphene oxide; PMMA nanocomposites; Controlled radical polymerization; ATRP

Background

The discovery of two-dimensional (2D) sp^2 hybridized graphene sheets by Novoselov [1] in 2004 has received much attention due to their extraordinary electrical, thermal, and mechanical properties [1-5]. Due to its high surface-area-to-volume ratio, graphene has been effectively used in the synthesis of polymer nanocomposites which exhibit enhanced physical and chemical properties over individual components [6]. The functionalization of graphene has received much attention in recent years as a way to improve interfacial interactions with other components, including organic and inorganic polymers, as the key to maximizing the end properties of the resulting graphene-polymer nanocomposites is controlling the dispersion of graphene within the matrix of the main components [7-9]. Moreover, the functional groups may not only improve the miscibility of graphene in organic solvents but also may provide nucleation sites for efficient *in situ* grafting of polymeric chains onto the graphene surface, which results in further improvements in mechanical and thermal properties [10].

Efforts to enhance the end properties of graphene-polymer nanocomposites using surface polymerization through *in situ* 'grafting to' and 'grafting from' techniques have been reported [11,12]. *In situ* polymerization offers the ability to control the polymer architecture and final morphology of the resulting composites. Ramanathan et al. reported an extraordinary shift in glass transition temperature (T_g), modulus, ultimate strength, and thermal stability for poly(acrylonitrile) and poly(methyl methacrylate) using very low levels of functionalized graphene sheets [13]. *In situ* emulsion polymerization of methyl methacrylate (MMA) was carried out by Kuila et al. using graphene as a reinforcing filler, which also enhanced the storage moduli, T_g , and thermal stability of the resulting nanocomposites [14].

Living ionic polymerization has been widely used to produce homo- and block copolymers with well-defined architectures, controlled molecular weights, and narrow polydispersity index (PDI). However, the industrial applications of ionic polymerization are limited due to the need for rigorous polymerization conditions, such as highly purified monomers and solvents. In addition, living ionic polymerization can only be used to polymerize hydrocarbon monomers and the polar monomer due to unwanted side reactions. Atom transfer radical polymerization (ATRP) is an alternative polymerization technique to

* Correspondence: shhur@ulsan.ac.kr
School of Chemical Engineering, University of Ulsan, Daehakro 93, Ulsan, Namgu 680-749, Korea

improve polymer architectures under simple polymerization conditions in the presence of hydrophilic organic/inorganic fillers such as layered silicates and graphene oxide (GO) [15,16]. The direct growth of thermoresponsive poly-2-(dimethylamino)ethyl methacrylate polymer brushes with narrow PDI through surface-initiated highly controlled ATRP from initiator functionalized graphene sheets has been reported, where the polymers were grown directly from a graphene surface with covalent functionalization to tune the physical, thermal, and electrical properties [17]. Pyrene-based functionalized graphene has been used for reversible addition fragmentation chain transfer (RAFT) polymerization of dimethyl aminoethyl acrylate, acrylic acid, and styrene in order to avoid graphene aggregation [18]. The efficient functionalization through diazotization of graphene for ATRP of styrene results in high-performance polymer-graphene nanocomposites with increased tensile strength, T_g and Young's modulus [19]. Covalently bounded polystyrene polymer chains have been systematically tuned using ATRP on single-layer graphene nanosheets by Fang et al. [20]. High-density grafted polymer-graphene nanocomposites exhibit an appreciable increase in T_g compared with low-density grafted samples.

In this study, we focused on the functionalization of GO and high-density grafting of poly(methyl methacrylate) (PMMA) chains onto its surface through an *in situ* 'grafting from' technique using ATRP. Quaternization and esterification after diazotization were carried out to increase the number of anchoring sites for ATRP initiators for increased grafting of polymer chains on the GO surface. ATRP of MMA was carried out using GO with ATRP initiators on the surface, cupric bromide (CuBr, catalyst), and N,N,N',N'',N''-pentamethyldiethylenetriamine (PMDETA, ligand) at ambient temperature. The resulting graphene-PMMA nanocomposites showed higher thermal stability and higher glass transition temperatures (T_g) than pristine PMMA polymers.

Methods

Acid-treated natural expandable graphite (grade 1721) was purchased from Asbury Carbons, Asbury, NJ, USA. Concentrated sulfuric acid (H₂SO₄), potassium permanganate (KMnO₄), sodium nitrate (NaNO₃), sodium nitrite (NaNO₂), sodium carbonate (Na₂CO₃), hydrochloric acid (HCl, 35%), hydrogen peroxide (H₂O₂, 30 wt.%), N, N'-dimethylformamide (DMF), MMA, 2-chloroethanol, *p*-aminobenzoic acid, and 2,2',2''-trihydroxy-triethylamine (triethanolamine) were purchased from Daejung Reagents & Chemicals, Ulsan, Korea. Cuprous bromide (CuBr), N, N,N',N'',N''-PMDETA and polystyrene standards for gel permeation chromatography (GPC) were purchased from Sigma-Aldrich, St. Louis, MO, USA and were used as

received without further purification. The stabilizing agent was removed from commercial MMA by washing three times with sodium hydroxide (NaOH), followed by vacuum distillation; the middle portion was stored at 0°C to 4°C until use. DMF was stirred with anhydrous calcium hydride (CaH₂) and then distilled before use.

Preparation of DGO-Br

The preparation steps of GO, diazotized GO (DGO-COOH), tetrakis(2-hydroxyethyl) ammonium chloride (THAC), DGO-COO⁻Na⁺, and DGO-OH have been reported in our previous paper [21]. DGO-Br was prepared by the esterification of α -bromoisobutyryl bromide with DGO-OH. In brief, 2 g of DGO-OH powder was dispersed in distilled dry DMF using sonication, and 1 mL of triethyl amine was added to the suspension under a nitrogen atmosphere. The α -bromoisobutyryl bromide was added slowly to the above suspension at 0°C using a gas-tight syringe. The reaction mixture was stirred at the same temperature for 6 h and then increased to 25°C and stirred for 12 h. The resulting suspension (DGO-Br) was centrifuged and washed repeatedly with acetone and methanol and dried at 65°C in a vacuum oven.

Polymerization of MMA on the surface of DGO-Br

The ATRP of MMA was carried out using the prepared DGO-Br. In a typical procedure, 30 mg of DGO-Br was dissolved in 5 mL of distilled dry DMF and was homogeneously dispersed by ultrasonication for 30 min before starting polymerization. Next, 15 mg of CuBr, 15 μ L of PMDETA catalyst, and 5 mL of MMA were added successively. The reaction mixture was then degassed three times and vacuum-sealed with a septum, followed by nitrogen purging for 30 min to evacuate the residual oxygen. The mixture was then placed in a thermo-stated oil bath at 80°C for the designated period of time. Polymerization was stopped by quenching the polymerization tube in ice cold water. The resulting solution was poured into a petri dish to evaporate the excess solvent. The polymerization yields were calculated gravimetrically.

Detachment of the polymer chains from the GO surface

To determine the molecular weight by GPC, polymeric chains were detached from the surface of DGO-Br through a reverse cation exchange process. In brief, the resulting graphene-PMMA nanocomposite (0.5 g) was dissolved in 50 mL of tetrahydrofuran (THF), and lithium chloride (0.05 g) was added to the reaction mixture. The solution was refluxed for 24 h and filtered through Celite (Sigma-Aldrich). The free polymer was recovered by adding the filtrate into methanol and was then filtered and dried in a vacuum oven.

Characterization

Raman spectra were recorded using a confocal Raman spectrometer (Alpha300S, WITec, Ulm, Germany) with a 633-nm wavelength incident laser light. The crystallographic structures of the materials were determined by a wide-angle X-ray diffraction (WAXRD) system (Rigaku RU-200 diffractometer, Shibuya-ku, Japan) equipped with a Ni-filtered Cu K α source (40 kV, 100 mA, $\lambda = 0.15418$ nm). Bragg's equation ($n\lambda = 2d\sin\theta$) was used to calculate the d spacing between the layers. X-ray photoelectron spectroscopy (XPS) was performed to determine the oxidation status of carbon using a Thermo Fisher X-ray photoelectron spectrophotometer (Waltham, MA, USA) employing an

Al K α X-ray source (1,486.6 eV). Thermogravimetric analysis (TGA) was performed to analyze the thermal behavior of the samples using a TGA analyzer (Q50, TA Instruments, New Castle, DE, USA) with a 10°C min⁻¹ heating rate in a nitrogen atmosphere. Number of average molecular weight (\bar{M}_n), weight average molecular weight (\bar{M}_w), and molecular weight distribution (MWD) were determined using a Waters GPC instrument (Milford, MA, USA) equipped with a 2414 differential refractive index detector and two (HR 2 and HR 4) Waters μ -Styragel columns. Spectral grade THF was used as an eluent at a flow rate of 1.0 ml min⁻¹, and the molecular weight calibrations were carried out using polystyrene standards.

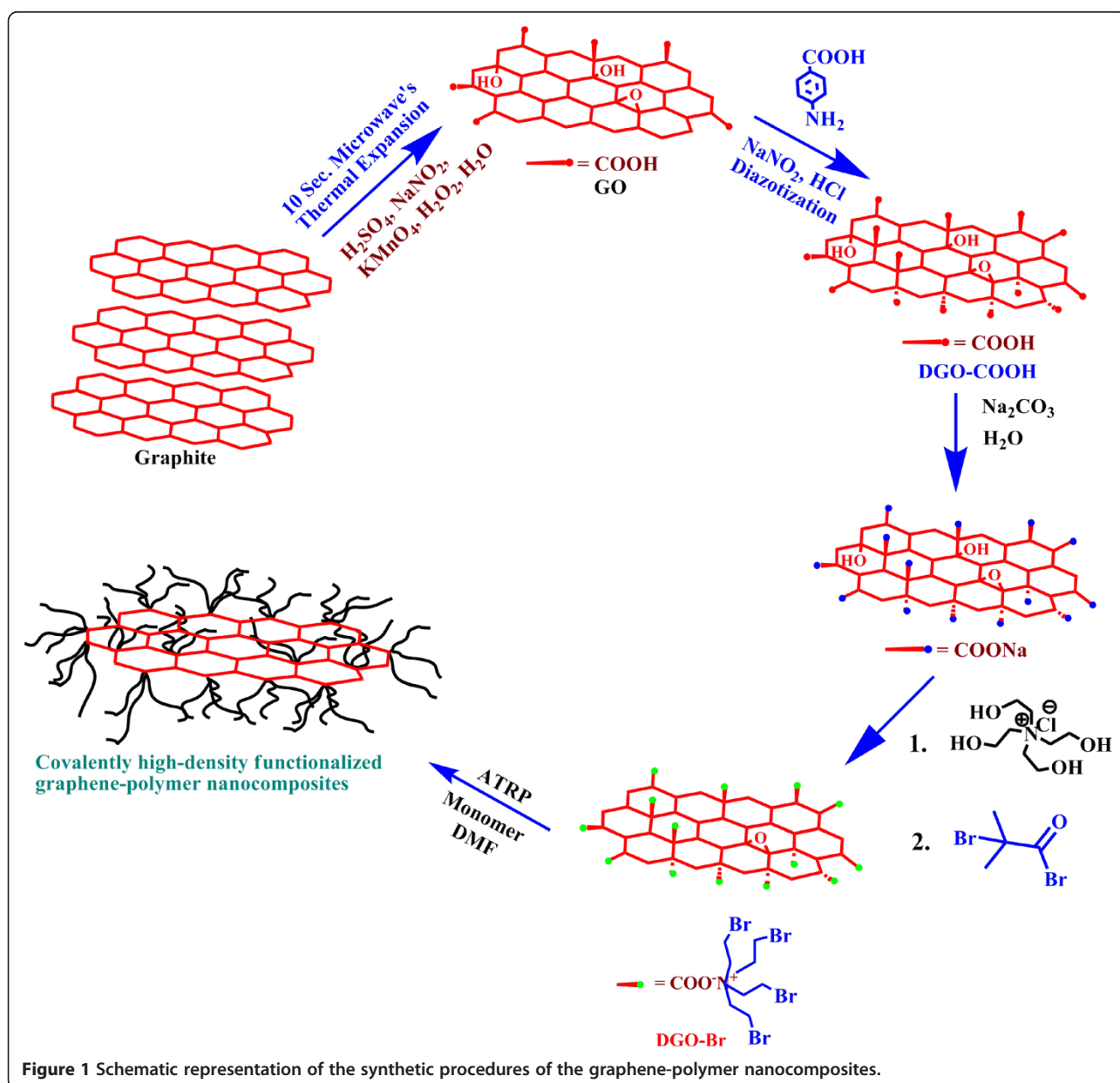


Figure 1 Schematic representation of the synthetic procedures of the graphene-polymer nanocomposites.

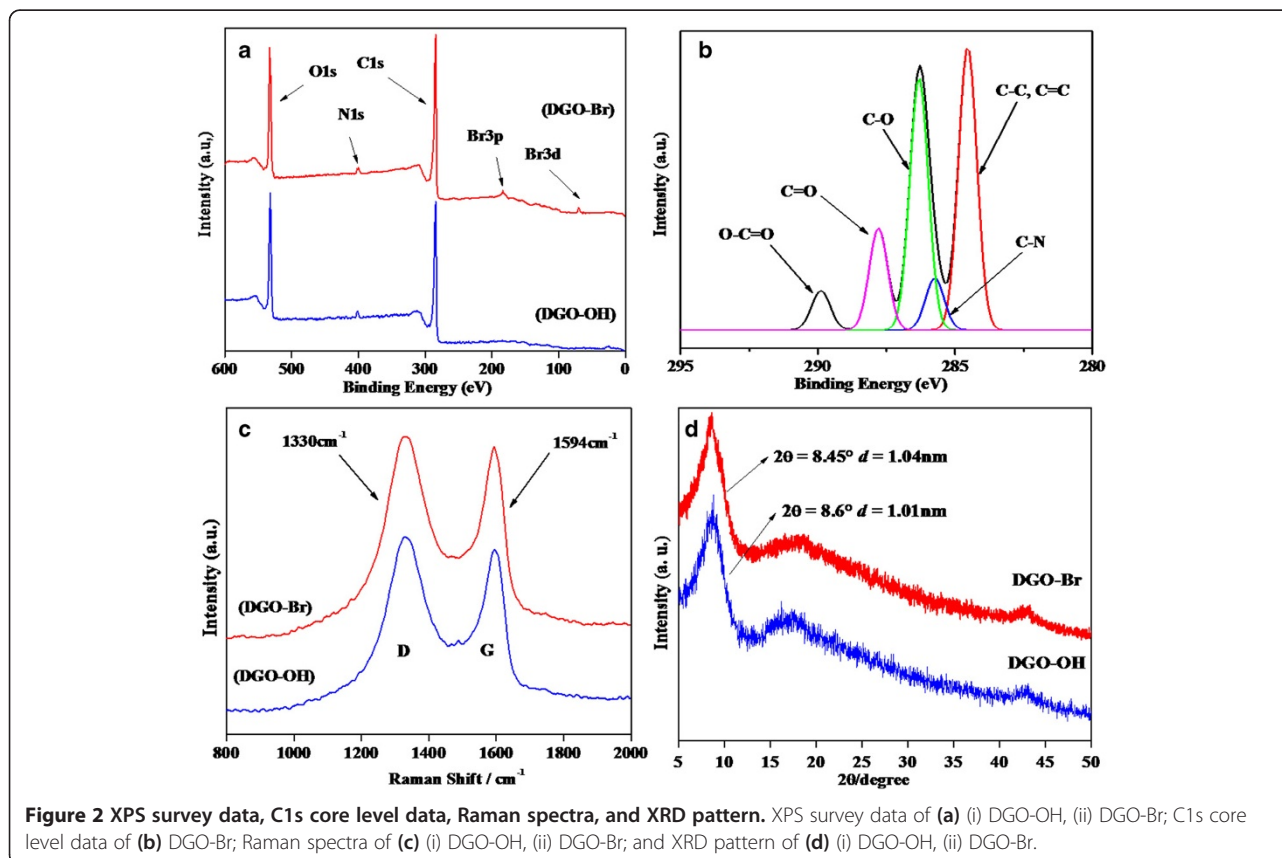
Results and discussion

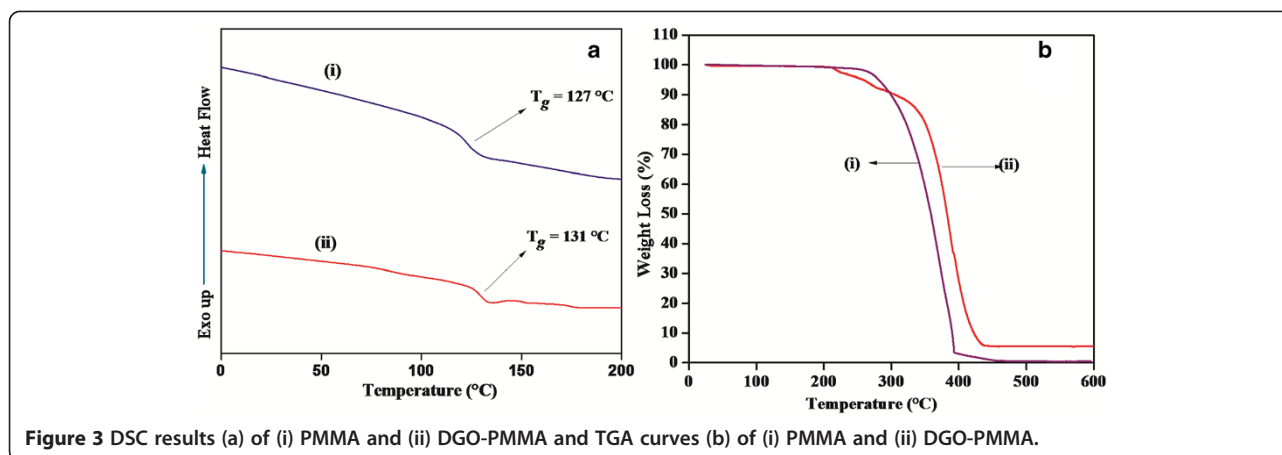
In general, good interaction between fillers and polymers leads to significant improvements in the properties of the resulting final products. To increase the interfacial interactions between GO and the polymers, the GO was first diazotized with *p*-aminobenzoic acid to obtain DGO-COOH, followed by a quaternization reaction with THAC and an esterification reaction with α -bromoisobutyryl bromide, which resulted in a tertiary bromine-terminated DGO-Br for efficient ATRP, as shown in Figure 1. Detailed characterizations of GO, DGO-COOH, and DGO-OH through FT-IR, Raman, XPS, XRD, and TGA have been reported in our previous paper [21]. In addition, XPS was used to investigate the changes in the functional groups of DGO-OH and DGO-Br, as shown in Figure 2a. Two intense peaks at 285 and 532 eV can be attributed to C1s and O1s, respectively [22]. The new peak of N1s at 399 to 400 eV was observed by diazotization. The C/O ratios of the functionalized DGO-OH and DGO-Br were 2.5 and 2.65, respectively, which can be correlated with dehydration during the esterification of DGO-OH to DGO-Br. The deconvoluted C1s XPS spectra of DGO-Br (Figure 2b) show several peaks at 284.5, 286.3, 287.9, and 289.7 eV originating from C-C, C-O, C=O, and O-C=O groups, respectively. In comparison to DGO-OH [21], the relative intensity of the C-C peak remains the same after esterification,

but the intensity of the C=O and O-C=O peaks increased, which may be due to increased functionality.

Raman spectra of DGO-OH and DGO-Br are shown in Figure 2c. The G and D bands in the Raman spectra originate from the first-order scattering of E_{2g} phonons of sp^2 -bonded carbon atoms and with a breathing mode of j -point photons of A_{1g} symmetry of sp^3 -bonded carbon atoms of disordered graphene. The Raman spectrum of DGO-OH shows sp^2 -bonded carbon stretching related to the G band at 1594 cm^{-1} and disordered, D band, sp^3 -bonded carbon atoms at 1330 cm^{-1} . The intensity ratio of the D and G bands (I_D/I_G) for DGO-OH and DGO-Br were 1.3 and 1.35, respectively. The slightly increased I_D/I_G ratio may be due to increased functionalization after esterification. WAXRD patterns of DGO-OH and DGO-Br are shown in Figure 2d. The DGO-OH and DGO-Br exhibit peaks at 8.6° and 8.45° , indicating d spacings of 1.01 nm and 1.04 nm, respectively (based on Bragg's equation). The slightly increased d spacing of DGO-Br over DGO-OH can be also attributed to the esterification of DGO-OH with α -bromoisobutyryl bromide.

Thermal properties of the graphene-PMMA nanocomposites were compared with pristine PMMA by differential scanning calorimetry (DSC) and TGA. Figure 3 shows the DSC and TGA results for pristine PMMA and graphene-PMMA nanocomposite (GP-5) samples. For DSC (Figure 3a),





the midpoints between the onset and offset points of the transition temperature were chosen as the T_g values. The graphene-PMMA nanocomposite showed a higher T_g than that of the pristine PMMA, which can be attributed to the interactions between GO and PMMA. The decomposition patterns for PMMA and GP-5 are shown in Figure 3b. About 15% of GP-5 nanocomposites decomposed between 130°C and 340°C, whereas pure PMMA decomposition started at 250°C. The initial decomposition of GP-5 may be due to the presence of additional labile functional groups after surface modification using quaternization followed by esterification onto the surface of GO [23]. On the other hand, the main decomposition of PMMA ends at 400°C, whereas that of the graphene-PMMA nanocomposite ends at 430°C. The difference in the thermal stability between pristine PMMA and GP-5 indicates that the presence of graphene layers improves the thermal properties of graphene-PMMA nanocomposites after *in situ* polymerization on the functionalized GO surface. The increased thermal stability of graphene-PMMA nanocomposites can be attributed to the attractive nature of graphene toward free radicals generated during decomposition as well as the tortuous path formation during the decomposition process [21,23].

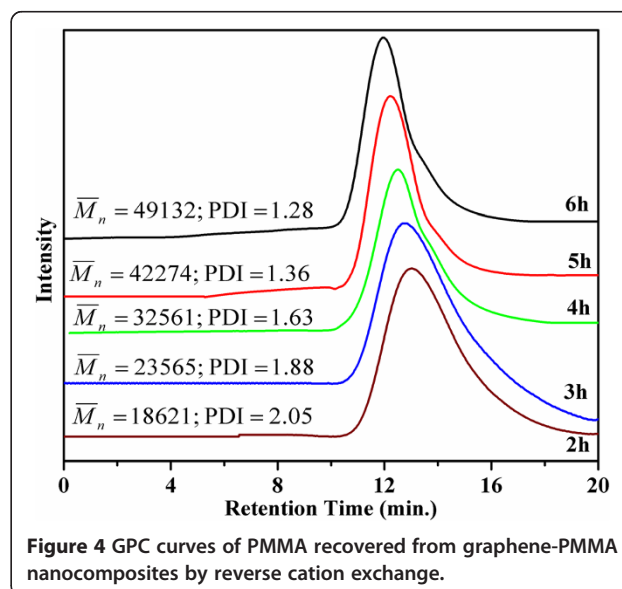
Table 1 Polymerization of MMA using TPEBMP at 80°C in DMF using DGO-Br

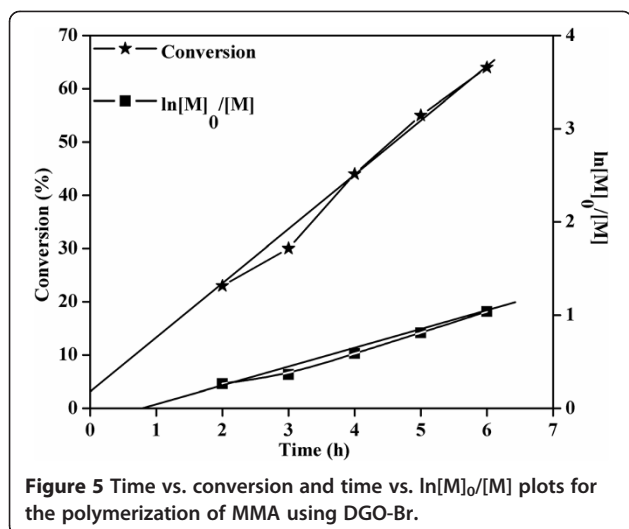
Code	Time (h)	^a Conversion (%)	GPC results		
			$\bar{M}_w \times 10^{-4}$	$\bar{M}_n \times 10^{-4}$	\bar{M}_w/\bar{M}_n
GP-1	2	23	3.8173	1.8621	2.05
GP-2	3	30	4.4302	2.3565	1.88
GP-3	4	44	5.3074	3.2561	1.63
GP-4	5	55	5.7492	4.2274	1.36
GP-5	6	64	6.2888	4.9132	1.28

^aConversion was determined gravimetrically.

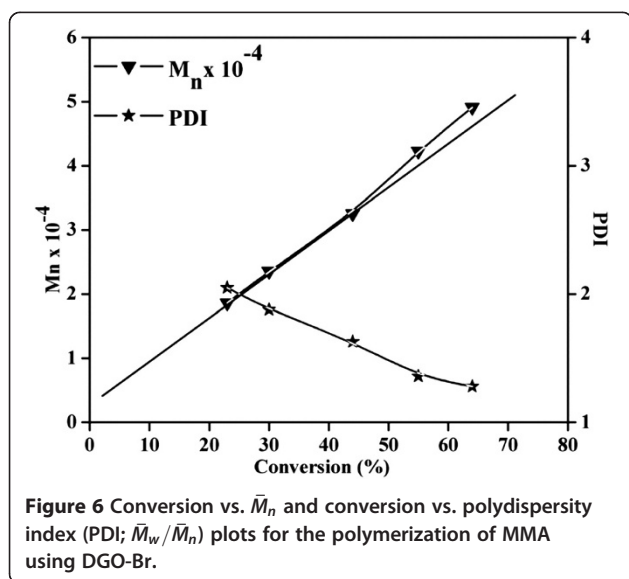
Controlled study of radical polymerization

Polymerization of MMA was carried out through ATRP using multifunctional DGO-Br, and controlled radical polymerization (CRP) was studied using GPC. The detailed GPC results (\bar{M}_n , \bar{M}_w , and MWD) are summarized in Table 1. As shown in Figure 4, as time increased, the GPC curves shifted from the lower molecular weight region to the higher molecular weight region due to the CRP mechanism. It is also interesting to note that the PDI values for PMMA become narrower with time, which also supports the CRP mechanism. Figure 5 shows the time vs. conversion and time vs. $\ln([M]_0/[M])$ plots for MMA polymerization, where $[M]_0$ and $[M]$ represent the initial monomer concentration and the monomer concentration at time t , respectively. The linear relation between time vs. $\ln([M]_0/[M])$ shows that the concentration of propagating radicals is





almost constant throughout the polymerization process. The small deviation in CRP results may be correlated with the induction period before starting the MMA polymerization, with similar results reported in previous literature [24,25]. As reported earlier, this induction period may account for the initial delay in reaching equilibrium between propagating radicals and dormant species. This delay may be responsible for the irreversible termination of some of the primary radicals in MMA polymerization, resulting in the deviations that are observed in the time vs. $\ln[M]_0/[M]$ plot. Further CRP was confirmed by plotting conversion against the number of average molecular weight (\bar{M}_n), as shown in Figure 6. A linear increase in molecular weight was observed with increasing monomer conversion, which confirms that the polymerization of MMA on the DGO-Br proceeds through the CRP



mechanism. The deviation of the conversion vs. \bar{M}_n plot is also correlated with slow initiation. These plots show that MMA polymerization undergoes an induction period with slow initiation, as reported previously [25].

Conclusions

ATRP initiator-attached high-density functionalized graphene oxide (DGO-Br) was prepared and used for MMA polymerization, resulting in graphene-PMMA nanocomposites through controlled radical polymerization. DSC and TGA studies show that the graphene-PMMA nanocomposites exhibited higher T_g and higher thermal stability compared to pristine PMMA polymers. GPC results confirmed the presence of a controlled radical polymerization mechanism using functionalized DGO-Br. We believe that high-density functionalized GO can be used to develop graphene-polymer nanocomposites with enhanced properties.

Competing interests

The authors declare that they have no competing interests.

Authors' contributions

MK has designed all the conducted experiments and characterization for final publication. JSC and SHH have approved the final manuscript. All authors read and approved the final manuscript.

Acknowledgements

This research was supported by the Basic Science Research Pro-gram through the National Research Foundation of Korea (NRF) funded by the Ministry of Education (2013R1A1A2A1004468).

Received: 13 February 2014 Accepted: 3 March 2014

Published: 10 July 2014

References

- Novoselov KS, Geim AK, Morozov SV, Jiang D, Zhang Y, Dubonos SV, Grigorieva IV, Firsov A: **Electric field effect in atomically thin carbon films.** *Science* 2004, **306**:666–669.
- Morozov SV, Novoselov KS, Katsnelson MI, Schedin F, Elias DC, Jaszczak JA, Geim AK: **Giant intrinsic carrier mobilities in graphene and its bilayer.** *Phys Rev Lett* 2008, **100**:016602.
- Balandin AA, Ghosh S, Bao W, Calizo I, Teweldebrhan D, Miao F, Lau CN: **Superior thermal conductivity of single-layer graphene.** *Nano Lett* 2008, **8**:902–907.
- Jang W, Chen Z, Bao W, Lau CN, Dames C: **Thickness-dependent thermal conductivity of encased graphene and ultrathin graphite.** *Nano Lett* 2010, **10**:3909–3913.
- Bunch JS, Zande AMVD, Verbridge SS, Frank IW, Tanenbaum DM, Parpia JM, Craighead HG, McEuen PL: **Electromechanical resonators from graphene sheets.** *Science* 2007, **315**:490–493.
- Huang X, Qi X, Boey F, Zhang H: **Graphene-based composites.** *Chem Soc Rev* 2012, **41**:666–686.
- Paulus GLC, Wang QH, Strano MS: **Covalent electron transfer chemistry of graphene with diazonium salts.** *Acc Chem Res* 2013, **46**:160–170.
- Kuila T, Bose S, Mishra AK, Khanra P, Kim NH, Lee JH: **Chemical functionalization of graphene and its applications.** *Prog Mater Sci* 2012, **57**:1061–1105.
- Georgakilas V, Otyepka M, Bourlinos AB, Chandra V, Kim N, Kemp KC, Hobza P, Zboril R, Kim KS: **Functionalization of graphene: covalent and non-covalent approaches: derivatives and applications.** *Chem Rev* 2012, **112**:6156–6214.
- Salavagione HJ, Martínez G, Ellis G: **Recent advances in the covalent modification of graphene with polymers.** *Macromol Rapid Comm* 2011, **32**:1771–1789.
- Badri A, Whittaker MR, Zetterlund PB: **Modification of graphene/graphene oxide with polymer brushes using controlled/living radical polymerization.** *J Polym Sci Part A: Polym Chem* 2012, **50**:2981–2992.

12. Ye YS, Chen YN, Wang J-S, Rick J, Huang YJ, Chang FC, Hwang ABJ: **Versatile grafting approaches to functionalizing individually dispersed graphene nanosheets using RAFT polymerization and click chemistry.** *Chem Mater* 2012, **24**:2987–2997.
13. Ramanathan T, Abdala AA, Stankovich S, Dikin DA, Herrera-Alonso M, Piner RD, Adamson DH, Schniepp HC, Chen X, Ruoff RS, Nguyen ST, Aksay IA, Prud'homme RK, Brinson AC: **Functionalized graphene sheets for polymer nanocomposites.** *Nat Nanotechnol* 2008, **3**:327–331.
14. Kuila T, Bose S, Khanra P, Kim NH, Rhee KY, Lee JH: **Characterization and properties of in-situ emulsion polymerized poly(methyl methacrylate)/graphene nanocomposites.** *Compos Part A* 2011, **42**:1856–1861.
15. Wang JS, Matyjaszewski K: **Living/controlled radical polymerization: transition-metal-catalyzed atom transfer radical polymerization in the presence of a conventional radical initiator.** *Macromolecules* 1995, **28**:7572–7573.
16. Yang Y, Wang J, Zhang J, Liu J, Yang X, Zhao H: **Exfoliated graphite oxide decorated by PDMAEMA chains and polymer particles.** *Langmuir* 2009, **25**:11808–11814.
17. Lee SH, Dreyer DR, An J, Velamakanni A, Piner RD, Park S, Zhu Y, Kim SO, Bielawski CW, Ruoff RS: **Polymer brushes via controlled, surface-initiated atom transfer radical polymerization (ATRP) from graphene oxide.** *Macromol Rapid Comm* 2010, **31**:281–288.
18. Cui L, Liu J, Wang R, Liu Z, Yang W: **A facile "graft from" method to prepare molecular-level dispersed graphene-polymer composites.** *J Polym Sci Part A: Polym Chem* 2012, **50**:4423–4432.
19. Fang M, Wang K, Lu H, Yang Y, Nutt S: **Covalent polymer functionalization of graphene nanosheets and mechanical properties of composites.** *J Mater Chem* 2009, **19**:7098–7105.
20. Fang M, Wang K, Lu H, Yang Y, Nutt S: **Single-layer graphene nanosheets with controlled grafting of polymer chains.** *J Mater Chem* 2010, **20**:1982–1992.
21. Kumar M, Chung JS, Kong BS, Kim EJ, Hur SH: **Synthesis of graphene-polyurethane nanocomposite using highly functionalized graphene oxide as pseudo-crosslinker.** *Mat Lett* 2013, **106**:319–321.
22. Liu J, Chen G, Jiang M: **Supramolecular hybrid hydrogels from noncovalently functionalized graphene with block copolymers.** *Macromolecules* 2011, **44**:7682–7691.
23. Goncalves G, Marques PAAP, Barros-Timmons A, Bdkin I, Singh MK, Emami N, Gracio J: **Graphene oxide modified with PMMA via ATRP as a reinforcement filler.** *J Mater Chem* 2010, **20**:9927–9934.
24. Kumar M, Kannan T: **A novel tertiary bromine-functionalized thermal iniferter for controlled radical polymerization.** *Polym J* 2010, **42**:916–922.
25. Qin DQ, Qin SH, Chen XP, Qiu KY: **Living controlled radical polymerization of methyl methacrylate by reverse ATRP with DCDPS/FeCl₃/PPh₃ initiating system.** *Polymer* 2000, **41**:7347–7352.

doi:10.1186/1556-276X-9-345

Cite this article as: Kumar et al.: Controlled atom transfer radical polymerization of MMA onto the surface of high-density functionalized graphene oxide. *Nanoscale Research Letters* 2014 **9**:345.

Submit your manuscript to a SpringerOpen[®] journal and benefit from:

- Convenient online submission
- Rigorous peer review
- Immediate publication on acceptance
- Open access: articles freely available online
- High visibility within the field
- Retaining the copyright to your article

Submit your next manuscript at ► springeropen.com